Highlights

Biosynthetic isotope fractionation negligibly impacts biomarker ^{14}C ages

Jordon D. Hemingway

- Acetogenic lipid biosynthesis follows mass-dependent carbon isotope fractionation
- Acetogenic lipid biosynthesis $^{14}C/^{13}C$ mass laws range from $b \approx 1.87$ to $b \approx 1.97$
- Non-canonical mass-laws are only expressed when ^{13}C fractionation is negligibly small
- Fractionation cannot explain anomalously old *n*-alkane ^{14}C ages

Biosynthetic isotope fractionation negligibly impacts biomarker ^{14}C ages

Jordon D. Hemingway[a,b,1,*]

[a]*Department of Earth and Planetary Sciences, Harvard University, Cambridge, MA, USA*
[b]*Geological Institute, Department of Earth Sciences, ETH Zürich, Zürich, Switzerland*

Abstract

Radiocarbon (^{14}C) ages of acetogenic lipid biomarkers such as *n*-alkanes are a powerful tool to track carbon-cycle turnover times. In sediments, biomarker ages are almost always older than the depositional age due to reservoir effects. Recently, Lane et al. [2021, Anomalously low radiocarbon content of modern *n*-alkanes, *Organic Geochemistry* **152**, 104170] reported ^{14}C ages up to ≈1500 yr for *n*-alkanes extracted from leaf tissue of living plants; they attributed this apparent "pre-aging" to biosynthetic fractionation against ^{14}C. However, reported ^{14}C ages are always corrected for mass-dependent fractionation using a ^{14}C/^{13}C mass law, b, of 2.0. Lane et al.'s interpretation therefore requires that lipid biosynthesis follows large, anomalous deviations from mass-dependent fractionation, with b reaching values as high as ≈ 124. Here, I test this assumption by estimating kinetic and equilibrium mass laws for various processes involved in acetogenic lipid biosynthesis using simple approximations and more robust computational chemistry methods. I find that kinetic b values range from 1.880 to 1.995 and that equilibrium b values for several chain elongation steps range from 1.856 to 1.880, consistent with previous results for other chemical and biological processes. In contrast, complex reaction networks may lead to large expressed b values, but only when net $\ln(^{13}\alpha) \rightarrow 0$. Combined, these results imply maximum ^{14}C age offsets due to biosynthetic fractionation of ∼ 20 to 40 yr. Biomarker ^{14}C ages are therefore robust to biosynthetic isotope fractionation and can be confidently interpreted to reflect carbon-cycle turnover times.

Keywords: radiocarbon, mass-dependent fractionation, biomarkers

1. Introduction

Natural-abundance radiocarbon (^{14}C) activity represents a powerful geochronometer, with applications ranging from tracking of various carbon-cycle turnover times and reservoir ages to precise and accurate dating of sediments and anthropological artifacts. The utility of radiocarbon comes from its ubiquity; ^{14}C is incorporated into all inorganic and organic carbon (OC) phases. Of particular interest here is ^{14}C age measurement of specific lipid compounds—termed "biomarkers"—extracted from complex OC mixtures. Because a given biomarker is produced by a particular

*Corresponding author
Email address: jhemingway@ethz.ch (Jordon D. Hemingway)

group of organisms or biosynthetic/chemical pathway, its ^{14}C age offers insight into specific carbon-cycle processes that cannot be elucidated by the bulk OC age, which integrates signals from multiple sources. Since the advent of this technique by Eglinton et al. (1996), ^{14}C ages of multiple biomarker classes—for example, acetogenic plant-waxes (*n*-alkanes, *n*-alcohols, and *n*-alkanoic acids), isoprenoid archaeal lipids, lignin phenols, and condensed aromatic hydrocarbons—have been utilized to elucidate a broad suite of carbon-cycle processes, including: soil carbon turnover times, both in modern settings and in response to past climatic perturbations (Eglinton et al., 2021; Hein et al., 2020; Hemingway et al., 2018; Smittenberg et al., 2006); permafrost thaw (Feng et al., 2013); condensed aromatic ("black") carbon cycling (Coppola et al., 2018); marine sediment chronologies (Eglinton et al., 1997; Pearson and Eglinton, 2000); and microbial metabolisms (Ingalls et al., 2006; Petsch et al., 2001); among others.

Like all geochronometers, the utility of biomarker radiocarbon requires that ^{14}C ages are unaffected by kinetic and equilibrium processes that fractionate carbon isotopes and thus exclusively reflect the time that has passed since each compound was biosynthesized (after accounting for temporal changes in atmospheric ^{14}C inventory). This is accomplished by the practice of correcting measured ^{14}C activity for isotope fractionation using concomitantly measured $^{13}C/^{12}C$ ratios and assuming that fractionation is mass dependent (e.g., Stuiver and Polach, 1977). Following Craig (1954), fractionation corrections typically use a $^{14}C/^{13}C$ mass law, here termed b, of 2.0; that is, reported ages inherently assume that ^{14}C fractionates exactly twice as much as ^{13}C for any given process since the $^{14}C/^{12}C$ mass difference is roughly double that of the $^{13}C/^{12}C$ mass difference. Early work estimated the $^{14}C/^{13}C$ mass laws for various kinetic and equilibrium chemical reactions both theoretically and experimentally (e.g., Bigeleisen, 1952; Bigeleisen and Wolfsberg, 1953; Bigeleisen, 1949; Stern and Vogel, 1971); nearly all processes measured to date are described by a mass law of $b \in (1.8, 2.0)$, here termed the "canonical range". Although most processes cluster around $b = 1.9$ rather than the *reference line* value of $b_{RL} = 2.0$ used when reporting radiocarbon ages, resulting age biases caused by this difference have been shown to be less than or near ^{14}C analytical uncertainty (Wigley and Muller, 1981; Stuiver and Robinson, 1974; Southon, 2011; Fahrni et al., 2017; Steier et al., 2004). Thus, deviations from b_{RL} are often ignored and reported ^{14}C ages are considered unbiased.

Despite this established practice, Lane et al. (2021) recently extracted long-chain *n*-alkanes from the leaves of living plants and found biomarker ^{14}C ages that are up to ≈1500 yr older than bulk leaf tissue. They argued against contamination by ^{14}C-free ("dead") carbon—for example from solvent extraction or chemical processing steps—and instead interpret this "pre-aging" as a result of large, anomalous fractionation against ^{14}C during lipid biosynthesis. Because of this, they conclude that biomarkers violate a fundamental assumption of the radiocarbon geochronometer and urge caution when interpreting their ^{14}C ages. If true, this result would represent a major setback to the burgeoning compound-specific radiocarbon field and would possibly invalidate several recent carbon-cycle insights that have been elucidated using biomarker ^{14}C age measurements. This interpretation therefore warrants critical examination.

Here, I evaluate the Lane et al. (2021) hypothesis by focusing specifically on the plausibility of calculated b values that would be required to explain these data. Because multiple-isotope analysis is an established practice for many light element systems (e.g., O, Si, S), there exist robust theoretical derivations for determining mass laws. Drawing

upon this theory, I estimate b values for several relevant kinetic and equilibrium reactions using both simple approximations as well as more robust computational chemistry approaches. I then explore how overall expressed isotope effects and mass laws may deviate from those calculated for elementary reactions when incorporated into a complex (enzymatic) reaction network such as acetogenic lipid biosynthesis. Given these results, I estimate that fractionation during lipid biosynthesis can only explain ^{14}C age offsets up to ≈40 yr and conclude that biomarker radiocarbon results can be confidently interpreted to reflect aging in the environment. I briefly offer alternative explanations to interpret the data of Lane et al. (2021).

Table 1: Compilation of bulk leaf tissue and non-blank-corrected acetogenic lipid (*n*-alkane, *n*-alkanoic acid) δ^{13}C and F^{14}C data from living plants, including calculated $^{13}\alpha$ values (calculated using Eq. 6) and mass-law b values (calculated using Eq. 7) that would be required to explain observed age offsets if they were driven purely by fractionation. References are: [1] = Lane et al. (2021), [2] = Eglinton et al. (1996).

Species	Compounds	F^{14}C		δ^{13}C (‰ VPDB)		$\ln\left(^{13}\alpha\right)$ ×1000 ‰	b	Ref.
		bulk leaf	lipid	bulk leaf	lipid			
L. styraciflua L.	*n*-alkanes[a]	1.003 ± 0.003[b]	0.868 ± 0.002	−31.4[c]	−34.7[c]	−3.4	44.5	1
M. varginiana L.	*n*-alkanes[a]	1.005[c]	0.815 ± 0.002	−27.5[c]	−31.3[c]	−3.9	55.3	1
Q. nigra L.	*n*-alkanes[a]	1.003 ± 0.003[b]	0.810 ± 0.007	−28.7[c]	−30.4[c]	−1.8	123.8	1
Q. virginiana Mill.	*n*-alkanes[a]	1.005[c]	0.923 ± 0.002	−29.3[c]	−32.7[c]	−3.5	26.2	1
A. Stricta Michx.	*n*-alkanes[a]	1.004[c]	0.866 ± 0.002	−14.1[c]	−25.2[c]	−11.3	15.1	1
D. sanguinalis L.	*n*-alkanes[a]	1.000[c]	0.937 ± 0.002	−29.8[c]	−36.3[c]	−6.7	11.6	1
C. argentea	*n*-C_{31} alkane[d]	0.887 ± 0.010	0.816 ± 0.011	−23.9[c]	−38.1[c]	−14.7	7.7	2
A. americana	*n*-$C_{16:0+18:0}$ FA[e]	1.098 ± 0.007	0.990 ± 0.021	−14.8[c]	−27.8 ± 0.5	−13.3	9.8	2

[a] Urea-adducted apolar lipid extract with no further separation or purification procedures; see Lane et al. (2021) for details.

[b] Value not reported; taken as average of all reported bulk leaf tissue values from Lane et al. (2021) ($\mu \pm 1\sigma$; n = 4).

[c] No uncertainty reported in original publication.

[c] Mass-weighted average of all reported replicates after preparatory column gas chromatography ($\mu \pm 1\sigma$; n = 3).

[c] Mass-weighted average of all individually reported *n*-$C_{16:0}$ and *n*-$C_{18:0}$ separated by preparatory column gas chromatography ($\mu \pm 1\sigma$; n = 2).

2. Theory and methods

2.1. Radiocarbon nomenclature and mass law calculations

I first define the nomenclature and mathematical relationships required to estimate mass laws. Following Stuiver and Polach (1977) and Reimer et al. (2004), radiocarbon activity is typically reported in "fraction modern" as

$$\mathrm{F}^{14}\mathrm{C} = \frac{A_{s,N}}{0.95 \times A_{Ox,N}}, \tag{1}$$

where $A = {}^{14}\mathrm{C}/\mathrm{C}$ is the $^{14}\mathrm{C}$ activity, s refers to the sample, Ox refers to the Ox-I oxalic acid standard, N indicates that both activities are normalized for isotope fractionation, and the scalar 0.95 is added by convention. To be consistent with stable isotope nomenclature, I let $A \approx {}^{14}\mathrm{R}$, where ${}^{14}\mathrm{R} = {}^{14}\mathrm{C}/{}^{12}\mathrm{C}$ is the $^{14}\mathrm{C}$ isotope ratio; this approximation is commonly applied and has a negligible impact on calculated radiocarbon ages (Fahrni et al., 2017). Then, by explicitly including the fractionation normalization of Reimer et al. (2004), Eq. 1 becomes

$$\mathrm{F}^{14}\mathrm{C} = \frac{{}^{14}\mathrm{R}_s}{{}^{14}\mathrm{R}_{Ox}} \left(\frac{0.975}{0.981}\right)^{b_{\mathrm{RL}}} \left(\frac{{}^{13}\mathrm{R}_{Ox}}{{}^{13}\mathrm{R}_s}\right)^{b_{\mathrm{RL}}}, \tag{2}$$

where b_{RL} is the reference line mass law; following Craig (1954), nearly all $\mathrm{F}^{14}\mathrm{C}$ values are reported using $b_{\mathrm{RL}} = 2.0$. The first parenthetical term in Eq. 2 reflects the convention that the sample and Ox-I are corrected to $\delta^{13}\mathrm{C} = -25\ ‰$ and $\delta^{13}\mathrm{C} = -19\ ‰$, respectively, where

$$\delta^{13}\mathrm{C} = \left({}^{13}\mathrm{R}/{}^{13}\mathrm{R}_{\mathrm{VPDB}} - 1\right) \times 1000‰, \tag{3}$$

${}^{13}\mathrm{R} = {}^{13}\mathrm{C}/{}^{12}\mathrm{C}$, VPDB is the Vienna Pee Dee Belemnite reference material, and $‰$ indicates "permil" notation. Finally, radiocarbon age in conventional $^{14}\mathrm{C}$ yr can be calculated as

$${}^{14}\mathrm{C\ yr} = -8033 \ln\left(\mathrm{F}^{14}\mathrm{C}\right). \tag{4}$$

Following Eq. 2, it is apparent that $^{14}\mathrm{C}$ age biases may arise from isotope fractionation if a given fractionation process is described by a mass law that deviates from $b_{\mathrm{RL}} = 2.0$. Mass laws for any kinetic or equilibrium fractionation process can be calculated following the relationship (Southon, 2011; Young et al., 2002):

$$b_{\mathrm{p/r}} = \frac{\ln\left({}^{14}\alpha_{\mathrm{p/r}}\right)}{\ln\left({}^{13}\alpha_{\mathrm{p/r}}\right)}, \tag{5}$$

where

$${}^{*}\alpha_{\mathrm{p/r}} = \frac{{}^{*}\mathrm{R_p}}{{}^{*}\mathrm{R_r}} \tag{6}$$

is the fractionation factor, $* = 13$ or 14 is the isotope of interest, "p" refers to the product compound, and "r" refers to the reactant compound. Fahrni et al. (2017) showed that the mass-law b value for any process can be determined so long as the product and reactant $\mathrm{F}^{14}\mathrm{C}$ and $\delta^{13}\mathrm{C}$ values are known. That is, combining Eqs. 2, 5, and 6 yields

$$b_{\mathrm{p/r}} = b_{\mathrm{RL}} + \frac{\ln\left(\mathrm{F}^{14}\mathrm{C_p}\right) - \ln\left(\mathrm{F}^{14}\mathrm{C_r}\right)}{\ln\left({}^{13}\alpha_{\mathrm{p/r}}\right)}. \tag{7}$$

Finally, Eqs. 4 and 7 can be combined to yield the $^{14}\mathrm{C}$ age offset due to fractionation:

$${}^{14}\mathrm{C\ yr\ offset\ (product - reactant)} = -8033 \ln\left({}^{13}\alpha_{\mathrm{p/r}}\right)\left(b_{\mathrm{p/r}} - b_{\mathrm{RL}}\right). \tag{8}$$

I use Eq. 7 and data reported in Table 2 of Lane et al. (2021) to estimate $b_{\mathrm{p/r}}$ values that would be required if their $^{14}\mathrm{C}$ offsets between bulk leaf tissue and *n*-alkanes were due to fractionation (Table 1). When bulk leaf tissue $\mathrm{F}^{14}\mathrm{C}$

is not reported (i.e., for the species *L. styraciflua* and *Q. nigra* L.), I assume $F^{14}C = 1.003 \pm 0.003$, the average of all reported values ($\mu \pm 1\sigma$; $n = 4$). I calculate ${}^{13}\alpha_{p/r}$ using reported $\delta^{13}C$ values determined by isotope ratio mass spectrometry rather than those measured by accelerator mass spectrometry (AMS). This is appropriate here because $F^{14}C$ is determined using concomitantly measured, AMS-derived ^{13}R and ^{14}R values (Eq. 2); any fractionation during AMS analysis is thus already accounted for (c.f., Fahrni et al., 2017). Similarly, I use Eq. 8 to calculate predicted fractionation age offsets for kinetic, equilibrium, and complex reaction network processes using all ${}^{13}\alpha_{p/r}$ and $b_{p/r}$ estimates determined in this study.

Table 2: Estimated b^{kin} values calculated using Eq. 9 with ${}^{x}n = {}^{x}M$ (i.e., ideal gas diffusion) and with ${}^{x}n = {}^{x}\mu$ (i.e., bond breaking to form a transition state) for a suite of compounds relevant to acetogenic lipid biosynthesis.

Compound	${}^{12}M$ (amu)	b^{kin}	
		${}^{x}n = {}^{x}M$	${}^{x}n = {}^{x}\mu$
acetic acid	66.06	1.982	1.909
malonic acid	108.04	1.987	1.914
pyruvic acid	92.04	1.986	1.913
acetyl-ACP[a]	452.26	1.994	1.920
acetyl-CoA	847.36	1.995	1.921
malonyl-ACP[a]	469.25	1.994	1.921
malonyl-CoA	891.35	1.995	1.922
acetoacetyl-ACP[a]	469.29	1.994	1.921
Acetyl-ACP enolate[a]	423.25	1.994	1.920
n-C_{16} alkanoic acid	288.44	1.993	1.919
n-C_{32} alkanoic acid	544.89	1.995	1.921
mean ± std. dev. (*n* = 11)		**1.992 ± 0.005**	**1.918 ± 0.004**

[a]Acyl Carrier Protein, truncated at phosphopantetheine group.

2.2. Kinetic mass law estimates

Following Young et al. (2002), kinetic fractionation mass laws can be estimated using the general formula:

$$b^{kin} = \frac{\ln\left({}^{12}n/{}^{14}n\right)}{\ln\left({}^{12}n/{}^{13}n\right)}, \tag{9}$$

where ${}^{x}n$ is some measure of the mass of a molecule containing isotope x; I have added the superscript *kin* to explicitly indicate these are kinetic b values. Equation 9 is derived from transition state theory (Bigeleisen, 1949); it ignores temperature dependence and assumes purely classical mechanics (although a similar relationship can be derived using Marcus theory for quantum bond vibrations; see Young et al., 2002). To explore the possible range of kinetic mass

laws associated with lipid biosynthesis, I apply Eq. 9 by calculating ${}^{x}n$ in two different ways: (i) ${}^{x}n = {}^{x}M$, the molecular mass of the compound of interest, and (ii) ${}^{x}n = {}^{x}\mu$, the reduced mass of the compound of interested, calculated as

$$ {}^{x}\mu = \frac{{}^{x}mM}{{}^{x}m + M}, \tag{10} $$

where ${}^{x}m$ is the atomic mass of a given carbon isotope (i.e., ${}^{x}m = 12$, 13, or 14 amu) and M is the (isotopically unsubstituted) mass of all other atoms bonded to the atom of interest (i.e., $M = {}^{x}M - {}^{x}m$). Case (i) represents diffusion of an ideal gas, whereas case (ii) represents the breaking of a bond to form a transition state; these should roughly represent upper- and lower-bounds, respectively, for b^{kin} values (Young et al., 2002). I calculate b for both cases for suite of compounds relevant to lipid biosynthesis (acetic acid, malonic acid, pyruvic acid, acetyl-ACP, acetyl-CoA, malonyl-ACP, malonyl-CoA, acetoacetyl-ACP, acetyl-ACP enolate, n-C_{16} and n-C_{32} alkanoic acids); these compounds were chosen to span broad M range, and resulting b variability should therefore be conservative. For all calculations, I assume the only isotopic substitution occurs at the atom of interest. Resulting b^{kin} ranges are shown in Fig. 1 and individual values are reported in Table 2.

Table 3: Estimated ${}^{*}\beta$ values for a suite of compounds relevant to acetogenic lipid biosynthesis calculated using Eq. 12 and reported at several physiologically relevant temperatures

Compound	$\ln\left({}^{13}\beta\right) \times 1000$			$\ln\left({}^{14}\beta\right) \times 1000$		
	0 °C	25 °C	50 °C	0 °C	25 °C	50 °C
pyruvic acid	179.77	157.97	142.35	335.99	295.06	265.75
acetyl-ACP[a]	158.90	139.56	125.72	296.44	260.22	234.33
acetyl-CoA	160.05	140.55	126.61	298.62	262.11	236.02
malonyl-ACP[a]	180.14	157.84	141.90	336.59	294.75	264.86
malonyl-CoA	180.94	158.54	142.52	338.07	296.05	266.03
acetoacetyl-ACP[a]	167.80	147.13	132.35	313.08	274.39	246.75
Acetyl-ACP enolate[a]	145.08	127.34	114.67	270.84	237.60	213.86

[a] Acyl Carrier Protein, truncated at phosphopantetheine group.

2.3. Equilibrium mass law estimates

The equilibrium mass law for the triple-carbon isotope system can be estimated as

$$ b^{eq} = \frac{\frac{1}{{}^{12}m} - \frac{1}{{}^{14}m}}{\frac{1}{{}^{12}m} - \frac{1}{{}^{13}m}} = 1.854, \tag{11} $$

where I have similarly added the superscript eq to explicitly indicate equilibrium b values. This relationship is derived from the quantum vibrational modes of the reduced partition function ratio (RPFR) assuming a harmonic oscillator

(Bigeleisen and Goeppert Mayer, 1947; Urey, 1947); it is unique to a given isotope system and can be interpreted as the high-temperature limit of equilibrium fractionation between ideal, monoatomic atoms (Young et al., 2002). Still, equilibrium fractionation between any two compounds at temperatures relevant to Earth-surface conditions may deviate from this value. Although several steps of the acetogenic lipid biosynthesis pathway are unidirectional and irreversible (Wakil, 1989; Pearson, 2014), determining equilibrium mass laws between all relevant compounds may nonetheless provide a useful limit to explore the possible range of expressed b values. To provide robust constraints on this range, I estimate b^{eq} values using RPFRs determined by density functional theory using the computational chemistry software Gaussian 16 (Frisch et al., 2016).

Briefly, RPFRs for any isotopologue can be determined following the Bigeleisen-Goeppert Mayer-Urey equation (Bigeleisen and Goeppert Mayer, 1947; Urey, 1947):

$$^{*}\beta(T) = \frac{s}{s^*} \prod_{i=1}^{3N-y} \frac{u_i^*(T)}{u_i(T)} \frac{e^{-u_i^*(T)/2}}{e^{-u_i(T)/2}} \frac{1 - e^{-u_i(T)}}{1 - e^{-u_i(T)^*}}, \tag{12}$$

where

$$u_i(T) = \frac{h\omega_i}{k_B T}, \tag{13}$$

h is Planck's constant, ω_i is the harmonic normal mode frequency for degree-of-freedom i, k_B is Boltzmann's constant, T is temperature in Kelvin, s is the rotational symmetry number, N is the number of atoms in the compound of interest, and $y = 5$ for linear molecules or $y = 6$ for nonlinear molecules. Here, $^{*}\beta$ is the RPFR multiplied by the rotational symmetry number ratio (typically, $s/s^* = 1$ since isotopic substitution often does not change rotational symmetry). Following Cao and Liu (2011), equilibrium fractionation factors can be calculated as

$$^{*}\alpha_{\mathrm{p/r}}^{eq} = \frac{^{*}\beta_{\mathrm{p}}}{^{*}\beta_{\mathrm{r}}}, \tag{14}$$

and b^{eq} values can then determined following Eq. 5.

Here, I determine ω_i values and calculate $^{*}\beta(T)$ for a suite of compounds relevant to lipid biosynthesis (acetyl-ACP, acetyl-CoA, malonyl-ACP, malonyl-CoA, acetoacetyl-ACP, acetyl-ACP enolate, pyruvic acid) using the B3LYP/6-31G(d) method and basis set (Lee et al., 1988; Francl et al., 1982). This method and basis set were chosen as a balance between accuracy and computational efficiency; they are a common choice for triple-isotope studies (e.g., Cao and Liu, 2011). All compound geometries were optimized in H_2O solvent using the C-PCM solvation method (Barone and Cossi, 1998); for all analyses, stationary points were found and no imaginary frequencies were observed, indicating proper convergence.

Reported $^{*}\beta(T)$ values represent the average of results calculated for single isotope substitutions at all relevant carbon positions (e.g., at the C1 and C2 positions of acetate-containing compounds), assuming all other atoms in the molecule are isotopically unsubstituted. This practice dampens the influence of any small geometric perturbations that may spuriously influence ω_i values; however, it yields results that cannot discern between site-specific isotope compositions such as the odd-over-even C position pattern observed by Monson and Hayes (1982). No attempt was

made to correct for anharmonic effects or computational basis-set scaling factors. These corrections may influence calculated $^{13}\alpha$ by several permil, but they have been shown to negligibly impact triple-isotope mass laws to due error cancellation (Cao and Liu, 2011). I therefore assume calculated b^{eq} values are robust. Results are shown in Fig. 1 and $^{*}\beta$ values are reported in Table 3 at several physiologically relevant temperatures.

2.4. *Expressed mass laws for complex reaction networks*

Finally, I explore the range of possible mass laws—and thus ^{14}C age offsets—that can be expressed by multi-step reaction networks. For example, consider the enzymatic decarboxylation of pyruvate by the pyruvate dehydrogenase complex to form acetyl-CoA, the building block for all acetogenic lipids (Pearson, 2014). This reaction has been shown to yield product acetyl-CoA that is depleted in ^{13}C relative to reactant pyruvate; it has thus been invoked to explain observed *n*-alkanoic acid ^{13}C depletion relative to bulk biomass (Monson and Hayes, 1982). Although the overall reaction is unidirectional and irreversible, for the purpose of predicting isotope fractionation factors it is useful to consider the reversible formation of a transition state (e.g., Bigeleisen, 1949; Bao et al., 2015). The reaction can then be written as

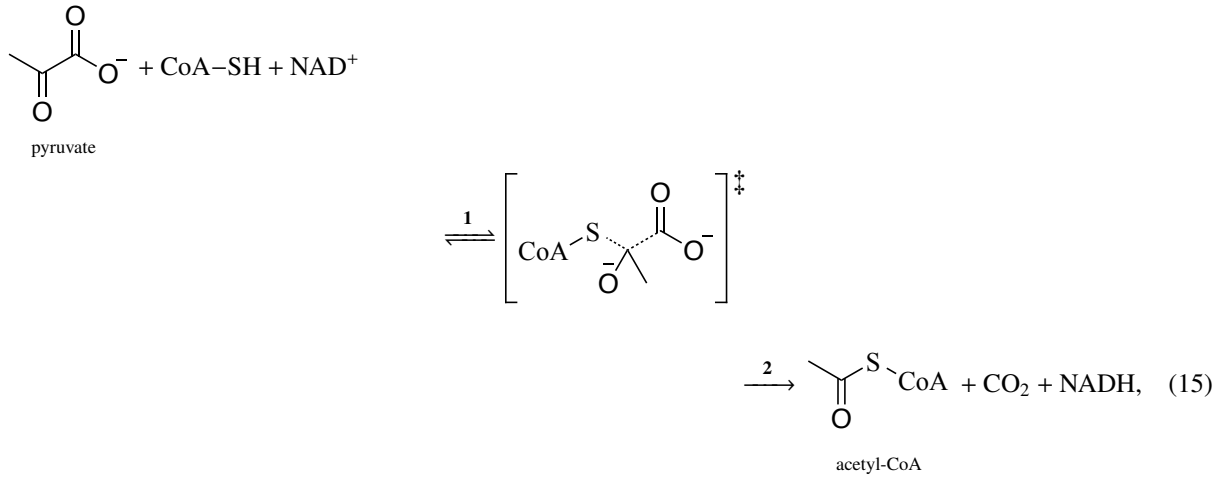

(15)

where ‡ represents the transition state. Equation 15 is a specific case of the general reaction network:

$$r \underset{}{\overset{\mathbf{1}}{\rightleftharpoons}} t \xrightarrow{\mathbf{2}} p, \tag{16}$$

where r is a reactant, t is a transition state, and p is a product. For a network of this form, Wing and Halevy (2014) showed that the net expressed fractionation factor can be written as

$$^{13}\alpha^{net}_{\mathrm{p/r}} = \left(^{13}\alpha^{k}_{2} \times {}^{13}\alpha^{eq}_{1} - {}^{13}\alpha^{k}_{1}\right) \times f + {}^{13}\alpha^{k}_{1}, \tag{17}$$

where subscripts 1 and 2 refer to the reaction steps in Eq. 15, superscripts k and eq refer to equilibrium or kinetic fractionation factors, and f reflects the degree to which reaction step **1** is reversible (i.e., the backward to forward flux ratio). Equation 17 can be similarly written for $^{14}\alpha^{net}_{\mathrm{p/r}}$ in terms of step-specific $^{13}\alpha$ and b values; the overall expressed

mass law, $b^{net}_{p/r}$, is then determined following Eq. 5. Several other lipid biosynthesis steps can be interpreted using a reaction pathway analogous to Eq. 16.

To investigate ^{14}C age offsets during acetyl-CoA formation, I solve Eq. 17 using a Monte Carlo approach. Specifically, I draw all input variables from uniform distributions assuming: $^{13}\alpha^{k}_{1} \in (0.985, 1.000)$, $^{13}\alpha^{k}_{2} \in (0.985, 1.000)$, $^{13}\alpha^{eq}_{1} \in (0.980, 1.020)$, $b^{k}_{1} \in (1.85, 2.00)$, $b^{k}_{2} \in (1.80, 2.00)$, $b^{eq}_{1} \in (1.86, 1.88)$, and $f \in (0, 1)$. These ranges were chosen for the following reasons: (i) kinetic $^{13}\alpha$ values for both steps encompass all observed plant-wax lipid fractionation factors in Chikaraishi et al. (2004), (ii) kinetic b values span the entire canonical range (Fig. 1; Stern and Vogel, 1971), (iii) equilibrium $^{13}\alpha$ and b values encompass the range calculated in Section 2.3 for all reaction pairs (Fig. 1), (iv) f spans the entire range from purely kinetic (unidirectional) to purely equilibrium (equal backward and forward fluxes). Resulting $^{13}\alpha^{net}_{p/r}$, $b^{net}_{p/r}$, and ^{14}C age offset ranges are therefore expected to be conservative estimates; true ranges are likely to be much narrower, particularly for $^{13}\alpha^{net}_{p/r}$ (e.g., Chikaraishi et al., 2004). Results for $n = 5000$ Monte Carlo draws are shown in Fig. 2.

3. Results and discussion

3.1. Predicted mass laws and age offsets

All kinetic b values calculated here fall within the canonical range, from a minimum of 1.909 to a maximum of 1.995 (Fig. 1; Table 2). Importantly, this includes predictions both for ideal gas molecular diffusion (calculated using molecular masses) and for bond breaking (calculated using reduced masses) for a suite of compounds ranging in size from acetic acid (66 amu) to malonyl-CoA (891 amu). In general, b predictions for diffusion (1.992 ± 0.005) are higher than those for bond breaking (1.918 ± 0.004). Although I do not expect any compounds involved in lipid biosynthesis to follow ideal gas diffusive behavior, it is nonetheless a useful limiting case to estimate maximum b^{kin} values. The observation that molecular diffusion approaches the reference line value ($b_{RL} = 2.0$) is consistent with a previously measured triple-oxygen mass law for O_2 diffusion of $b = 1.978$ (Yeung et al., 2012). Similarly, predicted b^{kin} values for bond breaking and transition-state formation are consistent with previous estimates for several abiotic S_N1, S_N2, E2, hydrogen transfer, and decarboxylation reactions (Stern and Vogel, 1971; Bigeleisen and Wolfsberg, 1953; Bigeleisen, 1952), as well as triple-oxygen and triple-sulfur kinetic mass laws expressed for several metabolic pathways (e.g., Wing and Halevy, 2014; Ash et al., 2020). Interestingly, measured mass laws for photosynthesis (1.953 ± 0.025; Fahrni et al., 2017) lie between the diffusion and bond-breaking scenarios calculated here, possibly reflecting the importance of CO_2 diffusion relative to that of isotope fractionation imparted by the RuBisCo enzyme (O'Leary, 1981). In general, I conclude that mass laws for all kinetic processes should lie within the canonical range.

Similarly, equilibrium b values calculated here for a suite of steps involved in acetogenic lipid biosynthesis all fall within a narrow range of 1.854 to 1.895 and exhibit only a small dependence on temperature (Fig. 1; Table 3). Although several of these steps are unidirectional and are thus not expected to operate in equilibrium in nature, these results again represent a useful limiting case to estimate minimum b values. For all studied reactions, $b^{eq}_{p/r}$

approaches the high-temperature, mono-atomic limit of $b = 1.854$ and is consistently lower than any calculated b^{kin} value. Computational chemistry results also yield ${}^{13}\alpha^{eq}_{\mathrm{p/r}}$ estimates (Fig. 1A), allowing one to predict the ^{14}C age offsets that would be imparted by these reactions (Eq. 8). In all cases, equilibrium isotope fractionation leads to a maximum age offset of ≈ 30 ^{14}C yr (Fig. 1C) despite the large range in predicted ${}^{13}\alpha^{eq}_{\mathrm{p/r}}$ values. This result confirms previous observations that small differences between measured b and b_{RL} will lead to small ^{14}C age biases even if ${}^{13}\alpha$ is large (Stuiver and Robinson, 1974; Southon, 2011; Fahrni et al., 2017). Similar to the b^{kin} case, I conclude that all equilibrium fractionation processes should lie within the canonical b range and that resulting ^{14}C age biases should be negligible.

In contrast to all b^{kin} and $b^{eq}_{\mathrm{p/r}}$ predictions, b^{net} values for multi-step reaction networks may reach non-canonical values much higher than 2.0 (Fig. 2C). However, Eq. 5 shows that non-canonical b values only manifest in the limiting case that $\ln\left({}^{13}\alpha^{net}_{\mathrm{p/r}}\right) \rightarrow 0$. For the simplified reaction network here (Eq. 15) this occurs when

$$ {}^{13}\alpha^{eq}_{1} \approx \frac{1 - {}^{13}\alpha^{k}_{1}\,(1-f)}{{}^{13}\alpha^{k}_{2} f}, \tag{18}$$

which can be accomplished either when $f = 0$ and ${}^{13}\alpha^{k}_{1} = 1.0$ or when $f \neq 0$ and ${}^{13}\alpha^{eq}_{1} > 1.0$ (assuming ${}^{13}\alpha^{k}_{1}$ and ${}^{13}\alpha^{k}_{2} < 1.0$). In general, large b^{net} values can manifest at so-called "crossover" points when one step of a reaction network is described by ${}^{13}\alpha > 1$ while another is described by ${}^{13}\alpha < 1$; this phenomenon has been observed previously both for triple-carbon and for triple-oxygen mass laws (Stern and Vogel, 1971; Bao et al., 2015). However, despite the potential for large b^{net} values, crossover points will not yield large ^{14}C age offsets since $\ln\left({}^{13}\alpha\right) \rightarrow 0$ (Eq. 8). That is, this large, non-canonical mass law is not expressed because carbon is not being isotopically fractionated. This can be seen in Fig. 2B, which shows that ^{14}C age offsets are always within $\approx \pm 40$ yr despite the large, conservative input parameter range and the possibility of crossover points.

Interestingly, this phenomenon may explain the one reliable documented experimental case that yielded $b > 2.0$—the two-step enzymatic hydrolysis of urea ($b = 3.17 \pm 0.38$; Schmitt et al., 1952). Several other experiments have reported $b > 2.0$, but these have largely been discredited as experimental artifacts (e.g., Southon, 2011); in contrast, the urea hydrolysis results are thought to be robust (Stern and Vogel, 1971). This reaction is known to follow a two-step pathway with a transition-state intermediate similar to the network shown in Eq. 16. If the corresponding ${}^{13}\alpha^{net}$ is sufficiently close to 1.0, then the observed b value could be the result of a crossover point. Other than this reaction, I know of no other biological process that has been reliably documented to yield triple-isotope mass laws outside of the canonical, mass-dependent range.

3.2. Are large biosynthetic ^{14}C age biases possible?

Given the range of kinetic, equilibrium, and net reaction mass laws observed here, it is possible to assess the claim made by Lane et al. (2021) that biosynthetic fractionation imparts ^{14}C age biases up to ≈1500 yr. In contrast to the large mass laws required for this hypothesis, I find that b values for all investigated kinetic and equilibrium fractionation process are within the canonical range of 1.8 to 2.0 (Fig. 1; Tables 2–3). Similarly, I show that large

expressed b values in multi-step reaction networks are only possible when overall fractionation trends to zero, thus imparting no appreciable age offset (Fig. 2). This finding is consistent with all literature mass-laws for biological and chemical processes for carbon, oxygen, and sulfur triple-oxygen isotope systems. Even when including experimental results that were subsequently disproven as artifacts (see e.g., Southon, 2011), I am unaware of any literature b value for the triple-carbon isotope system above ≈ 5 (Stern and Vogel, 1971); this is $\approx 2\times$ lower than the minimum value and $\approx 60\times$ lower than the maximum value required to explain the results of Lane et al. (2021). In contrast, so-called "mass-independent" fractionation—which has been observed in the triple-oxygen and triple-sulfur isotope systems—would lead to $b \approx 1.0$ (e.g., Thiemens and Lin, 2021). Still, this phenomenon is limited to gas-phase species in which an isotope substitution imparts asymmetry, which doubles the accessible rotational states compared to the symmetric isotopologue (Thiemens and Lin, 2021; Young et al., 2002). This is not the case for the reactions considered here. I thus conclude that b values for all steps during lipid biosynthesis fall within the canonical range and that isotope fractionation cannot explain large apparent ^{14}C age offsets.

Furthermore, Lane et al. (2021) hypothesize that differences in observed ^{14}C age offsets imply species-specific biosynthetic mass laws, further complicating the interpretation of biomarker ^{14}C ages. However, this interpretation would require an unprecedented level of biosynthetic mass-law variability, particularly between species within the C_3 angiosperms (b ranging from 26.2 to 123.8; Table 1). Even if b values as high as 123.8 were possible, this species-specific variability is highly suspect for several reasons.

First, although many proteins are involved in the overall biosynthesis of acetogenic lipids, several steps occur in different subunits of the multi-enzyme fatty acid synthase protein, which is highly conserved (Wakil, 1989). In particular, the amino acid sequences involved in the ester binding of acetyl and malonyl groups exhibit high homology across multiple domains of life (Yang et al., 1988; Wakil, 1989); these (reversible) binding steps ensure substrate entry into the subsequent synthesis cascade. Such high sequence homology therefore implies that this critical step of the biosynthetic pathway will exhibit similar active-site structure and thus similar fractionation factors and mass laws across all species.

Second, even if fatty acid synthase active sites between species are variable—or if a different, less conserved enzyme imparts the observed isotope fractionation—the range of b values invoked here is inconsistent with inter-species net mass-law variability observed for other multiple-isotope systems. For example, Wing and Halevy (2014) observe $^{33}\lambda$ values ranging from 0.506 to 0.516 (equivalent to $b = 1.94$ to 1.98 in the nomenclature used here) for different sulfate reducing bacteria under different nutrient conditions, even as $^{34}\alpha$ values exhibit large variability. Similarly, Ash et al. (2020) describe $^{17}\theta$ values between 0.523 and 0.525 (equivalent to $b = 1.90$ to 1.91) for different O_2-binding enzymes involved in oxic respiration. In addition to being within the canonical mass-law ranges for triple-sulfur and triple-oxygen isotope fractionation, observed variability in both of these studies is three orders of magnitude smaller than the range in species-specific b values invoked by Lane et al. (2021).

Finally, large b variability may be possible at the $^{13}\alpha$ crossover point; however, all ^{13}C fractionations reported in Lane et al. (2021) are far from this point (Fig. 2). Although the reaction network used here is highly simplified,

solutions to Eq. 15 suggests that b cannot exceed $\approx$ 2.4 within the observed $^{13}\alpha_{\text{lipid/leaf}}$ range (Fig. 2C). A more complicated reaction network is unlikely to invalidate this result. Interestingly, Chikaraishi et al. (2004) do observe C_3 angiosperms with *n*-alkanoic acid $\delta^{13}C$ values similar to—or slightly higher than—bulk leaf tissue $\delta^{13}C$, suggesting that acetogenic lipid biosynthesis near the crossover point may be possible. Nonetheless, I emphasize that this phenomenon will not impart an appreciable ^{14}C age offset since $\ln\left(^{13}\alpha\right) \rightarrow 0$ at the crossover point (Eq. 8; Fig. 2B).

Thus, the claim that different plant species will biosynthesize acetogenic lipids following highly variable b values is inconsistent with the known biochemistry of fatty acid production, enzymatic isotope fractionations, and all other observed biological mass laws—with a possible exception at the ^{13}C crossover point, where no ^{14}C age offset is expressed.

3.3. Interpreting anomalously old ^{14}C ages

Because biosynthetic fractionation cannot explain the anomalously old ^{14}C ages observed in Lane et al. (2021), this result must instead reflect incorporation of ^{14}C-depleted contaminant carbon. Similar biomarker age offsets have been observed previously and have been interpreted to reflect contamination by petrochemicals such as gas chromatography column bleed, residual solvent, urea, etc., during sample preparation (Table 1; Eglinton et al., 1996; Cisneros-Dozal et al., 2016). Many of these contaminants are removed by preparatory-column gas chromatography, which is typically utilized when isolating individual compounds for ^{14}C analysis (Eglinton et al., 1996); however, this method was not employed by Lane et al. (2021). Interestingly, Lane et al. (2021) considered but ultimately dismissed possibility that their results reflect ^{14}C-depleted blank contributions since their sample preparation procedure was careful to avoid possible contamination steps. However, no thorough blank assessment was performed. For example, previous blank assessment studies using the "modern-dead" isotope dilution approach—in which deviations from accepted $F^{14}C$ values for a suite of known standards are measured—have revealed large and variable contaminations, particularly for small samples and individual compounds (Santos et al., 2010). A similar blank assessment for the sample preparation procedure used in Lane et al. (2021) would be highly informative.

One plausible alternative explanation may be fossil-fuel derived deposition. Although Lane et al. (2021) were careful to avoid sampling near population centers, their sample site is $\approx$40 km from the 1600 MW coal-fired Weatherspoon Power Plant, which is known to emit aerosols via cooling towers (USDOE, 2007). Aerosol deposition on plant leaves is well documented (Wedding et al., 1975); if deposited aerosols are rich in apolar and aliphatic compounds, then this deposition may survive aqueous cleaning steps and impact the extracted *n*-alkanes while having a minor or negligible impact on bulk leaf tissue ^{14}C ages. Still, this explanation remains speculative.

4. Conclusions and outlook

Simple mass-law approximations and computational chemistry results indicate that each investigated step of the *n*-alkanoic acid biosynthetic pathway is described by canonical kinetic and equilibrium b values between 1.8 and 2.0,

consistent with all previously reported biological and chemical processes (e.g., Fahrni et al., 2017; Southon, 2011; Bigeleisen and Wolfsberg, 1953; Bigeleisen, 1949; Stern and Vogel, 1971). Using a simplified reaction network, I show theoretically that non-canonical b values can be expressed for multi-step (enzymatic) reactions such as n-alkanoic acid biosynthesis, but only at "crossover" points when $\ln(^{13}\alpha^{net}_{\mathrm{p/r}}) \rightarrow 0$. This behavior has been shown previously for several isotope systems (Stern and Vogel, 1971; Bao et al., 2015), and it may explain the only reliable, experimentally determined, non-canonical ^{14}C mass law reported in the literature—the two-step enzymatic hydrolysis of urea ($b = 3.17 \pm 0.38$; Schmitt et al., 1952). Because large b requires $\ln(^{13}\alpha^{net}_{\mathrm{p/r}}) \approx 0$, fractionation leads to maximum ^{14}C age offsets on the order of decades, similar to the ^{14}C analytical uncertainty. I therefore conclude that biomarker ^{14}C ages are robust to isotope fractionation during biosynthesis and that they can be confidently interpreted as a tracer for storage and turnover time in the environment after proper blank correction.

Acknowledgements

I thank Kevin Sutherland, Valier Galy, Ann McNichol, Tim Eglinton, Rienk Smittenberg, and the WHOI and ETH Radiocarbon Reading Groups for helpful and thought-provoking discussions related to this topic. The computations in this paper were run on the FASRC Cannon cluster supported by the FAS Division of Science Research Computing Group at Harvard University. No funding was provided for this work.

References

Ash, J.L., Hu, H., Yeung, L.Y., 2020. What fractionates oxygen isotopes during respiration? insights from multiple isotopologue measurements and theory. ACS Earth and Space Chemistry 4, 50–66.

Bao, H., Cao, X., Hayles, J.A., 2015. The confines of triple oxygen isotope exponents in elemental and complex mass-dependent processes. Geochimica et Cosmochimica Acta 170, 39–50.

Barone, V., Cossi, M., 1998. Quantum calculation of molecular energies and energy gradients in solution by a conductor solvent model. Journal of Physical Chemistry A 102, 1995–2001.

Bigeleisen, J., 1949. The relative reaction velocities of isotopic molecules. Journal of Chemical Physics 17, 675–678.

Bigeleisen, J., 1952. The effects of isotopic substitution on the rates of chemical reactions. Journal of Physical Chemistry 56, 823–828.

Bigeleisen, J., Goeppert Mayer, M., 1947. Calculation of equilibrium constants for isotopic exchange reactions. Journal of Chemical Physics 15, 261–267.

Bigeleisen, J., Wolfsberg, M., 1953. Fractionation of the carbon isotopes in decarboxylation reactions. VI. Comparison of the intermolecular isotope effects of a pair of isotopic isomers. Journal of Chemical Physics 21, 2120–2121.

Cao, X., Liu, Y., 2011. Equilibrium mass-dependent fractionation relationships for triple oxygen isotopes. Geochimica et Cosmochimica Acta 75, 7435–7445.

Chikaraishi, Y., Naraoka, H., Poulson, S.R., 2004. Hydrogen and carbon isotopic fractionations of lipid biosynthesis among terrestrial (C3, C4 and CAM) and aquatic plants. Phytochemistry 65, 1369–1381.

Cisneros-Dozal, L., Xu, X., Bryant, C., Pearson, E., Dungait, J., 2016. Grass material as a modern process standard for ^{14}C analysis of n-alkanes. Radiocarbon 58, 445–458.

Coppola, A.I., Wiedemeier, D.B., Galy, V., Haghipour, N., Hanke, U.M., Nascimento, G.S., Usman, M., Blattmann, T.M., Reisser, M., Freymond, C.V., Zhao, M., Voss, B., Wacker, L., Schefuß, E., Peucker-Ehrenbrink, B., Abiven, S., Schmidt, M.W., Eglinton, T.I., 2018. Global-scale evidence for the refractory nature of riverine black carbon. Nature Geoscience 11, 584–588.

Craig, H., 1954. Carbon 13 in plants and the relationships between carbon 13 and carbon 14 variations in nature. Journal of Geology 62, 115–149.

Eglinton, T.I., Aluwihare, L.I., Bauer, J.E., Druffel, E.R., McNichol, A.P., 1996. Gas chromatographic isolation of individual compounds from complex matrices for radiocarbon dating. Analytical Chemistry 68, 904–912.

Eglinton, T.I., Benitez-Nelson, B.C., Pearson, A., McNichol, A.P., Bauer, J.E., Druffel, E.R., 1997. Variability in radiocarbon ages of individual organic compounds from marine sediments. Science 277, 796–799.

Eglinton, T.I., Galy, V.V., Hemingway, J.D., Feng, X., Bao, H., Blattmann, T.M., Dickens, A.F., Gies, H., Giosan, L., Haghipour, N., Hou, P., Lupker, M., McIntyre, C.P., Montluçon, D.B., Peucker-Ehrenbrink, B., Ponton, C., Schefuß, E., Schwab, M.S., Voss, B.M., Wacker, L., Wu, Y., Zhao, M., 2021. Climate control on terrestrial biospheric carbon turnover. Proceedings of the National Academy of Sciences 118, e2011585118.

Fahrni, S.M., Southon, J.R., Santos, G.M., Palstra, S.W., Meijer, H.A., Xu, X., 2017. Reassessment ofo the $^{13}C/^{12}C$ and $^{14}C/^{12}C$ isotopic fractionation ratio and its impact on high-precision radiocarbon dating. Geochimica et Cosmochimica Acta 213, 330–345.

Feng, X., Vonk, J.E., van Dongen, B.E., Gustafsson, Ö., Semiletov, I.P., Dudarev, O.V., Wang, S., Montluçon, D.B., Wacker, L., Eglinton, T.I., 2013. Differential mobilization of terrestrial carbon pools in Eurasian Arctic river basins. Proceedings of the National Academy of Sciences 110, 14168–14173.

Francl, M.M., Pietro, W.J., Hehre, W.J., Binkley, J.S., Gordon, M.S., DeFrees, D.J., Pople, J.A., 1982. Self-consistent molecular orbital methods. XXIII. A polarization-type basis set for second-row elements. Journal of Chemical Physics 77, 3654–3665.

Frisch, M.J., Trucks, G.W., Schlegel, H.B., Scuseria, G.E., Robb, M.A., Cheeseman, J.R., Scalmani, G., Barone, V., Petersson, G.A., Nakatsuji, H., Li, X., Caricato, M., Marenich, A.V., Bloino, J., Janesko, B.G., Gomperts, R., Mennucci, B., Hratchian, H.P., Ortiz, J.V., Izmaylov, A.F., Sonnenberg, J.L., Williams-Young, D., Ding, F., Lipparini, F., Egidi, F., Goings, J., Peng, B., Petrone, A., Henderson, T., Ranasinghe, D., Zakrzewski, V.G., Gao, J., Rega, N., Zheng, G., Liang, W., Hada, M., Ehara, M., Toyota, K., Fukuda, R., Hasegawa, J., Ishida, M., Nakajima, T., Honda, Y., Kitao, O., Nakai, H., Vreven, T., Throssell, K., Montgomery, Jr., J.A., Peralta, J.E., Ogliaro, F., Bearpark, M.J., Heyd, J.J., Brothers, E.N., Kudin, K.N., Staroverov, V.N., Keith, T.A., Kobayashi, R., Normand, J., Raghavachari, K., Rendell, A.P., Burant, J.C., Iyengar, S.S., Tomasi, J., Cossi, M., Millam, J.M., Klene, M., Adamo, C., Cammi, R., Ochterski, J.W., Martin, R.L., Morokuma, K., Farkas, O., Foresman, J.B., Fox, D.J., 2016. Gaussian 16 Revision C.01. Gaussian Inc. Wallingford CT.

Hein, C.J., Usman, M., Eglinton, T.I., Haghipour, N., Galy, V.V., 2020. Millennial-scale hydroclimate controls of tropical soil carbon storage. Nature 581, 63–66.

Hemingway, J.D., Hilton, R.G., Hovius, N., Eglinton, T.I., Haghipour, N., Wacker, L., Chen, M.C., Galy, V.V., 2018. Microbial oxidation of lithospheric organic carbon in rapidly eroding tropical mountain soils. Science 360, 209–212.

Ingalls, A.E., Shah, S.R., Hansman, R.L., Aluwihare, L.I., Santos, G.M., Druffel, E.R., Pearson, A., 2006. Quantifying archaeal community autotrophy in the mesopelagic ocean using natural radiocarbon. Proceedings of the National Academy of Sciences 103, 6442–6447.

Lane, C.S., Yanuskiewicz, E.A., Mead, R.N., Horn, S.P., 2021. Anomalously low radiocarbon content of modern *n*-alkanes. Organic Geochemistry 152, 104170.

Lee, C., Yang, W., Parr, R.G., 1988. Development of the Colle-Salvetti correlation-energy formula into a functional of the electron density. Physical Review B 37, 785–789.

Monson, K.D., Hayes, J.M., 1982. Carbon isotopic fractionation in the biosynthesis of bacterial fatty acids. Ozonolysis of unsaturated fatty acids as a means of determining the intramolecular distribution of carbon isotopes. Geochimica et Cosmochimica Acta 46, 139–149.

O'Leary, M.H., 1981. Carbon isotope fractionation in plants. Phytochemistry 20, 553–567.

Pearson, A., 2014. Lipidomics for geochemistry. Treatise on Geochemistry 12, 291–336.

Pearson, A., Eglinton, T.I., 2000. The origin of *n*-alkanes in Santa Monica Basin surface sediment: a model based on compound-specific $\Delta^{14}C$ and $\delta^{13}C$ data. Organic Geochemistry 31, 1103–1116.

Petsch, S.T., Eglinton, T.I., Edwards, K.J., 2001. ^{14}C-dead living biomass: evidence for microbial assimilation of ancient organic carbon during shale weathering. Science 292, 1127–1131.

Reimer, P.J., Brown, T.A., Reimer, R.W., 2004. Discussion: reporting and calibration of post-bomb ^{14}C data. Radiocarbon 46, 1299–1304.

Santos, G.M., Southon, J.R., Drenzek, N.J., Ziolkowski, L.A., Druffel, E., Xu, X., Zhang, D., Trumbore, S., Eglinton, T.I., Hughen, K.A., 2010.

Blank assessment for ultra-small radiocarbon samples: chemical extraction and separation versus AMS. Radiocarbon 52, 1322–1335.

Schmitt, J.A., Myerson, A.L., Daniels, F., 1952. Relative rates of hydrolysis of urea containing C^{14}, C^{13}, and C^{12}. Journal of Physical Chemistry 56, 917–920.

Smittenberg, R.H., Eglinton, T.I., Schouten, S., Sinninghe Damsté, J.S., 2006. Ongoing buildup of refractory organic carbon in boreal soils during the Holocene. Science 314, 1283–1286.

Southon, J., 2011. Are the fractionation corrections correct: are the isotopic shifts for $^{14}C/^{12}C$ ratios in physical processes and chemical reactions really twice those for $^{13}C/^{12}C$? Radiocarbon 53, 691–704.

Steier, P., Dellinger, F., Kutschera, W., Priller, A., Rom, W., Wild, E.M., 2004. Pushing the precision limit of ^{14}C AMS. Radiocarbon 46, 5–16.

Stern, M.J., Vogel, P.C., 1971. Relative ^{14}C–^{13}C kinetic isotope effects. Journal of Chemical Physics 55, 2007–2013.

Stuiver, M., Polach, H.A., 1977. Discussion: Reporting of ^{14}C data. Radiocarbon 19, 355–363.

Stuiver, M., Robinson, S.W., 1974. University of Washington Geosecs North Atlantic carbon-14 results. Earth and Planetary Science Letters 23, 87–90.

Thiemens, M.H., Lin, M., 2021. Discoveries of mass independent isotope effects in the solar system: past, present, and future. Reviews in Mineralogy & Geochemistry 86, 35–95.

Urey, H.C., 1947. The thermodynamic properties of isotopic substances. Journal of the Chemical Society , 562–581.

USDOE, 2007. The National Energy Technology Laboratory 2007 coal power plant database. Technical Report. United States Department of Energy.

Wakil, S.J., 1989. Fatty acid synthase, a proficient multifunctional enzyme. Biochemistry 28, 4523–4530.

Wedding, J.B., Carlson, R.W., Stukel, J.J., Bazzaz, F., 1975. Aerosol deposition on plant leaves. Environmental Science & Technology 9, 151–153.

Wigley, T., Muller, A., 1981. Fractionation corrections in radiocarbon dating. Radiocarbon 23, 173–190.

Wing, B.A., Halevy, I., 2014. Intracellular metabolite levels shape sulfur isotope fractionation during microbial sulfate reduction. Proceedings of the National Academy of Sciences 111, 18116–18125.

Yang, C.Y., Huang, W.Y., Chirala, S., Wakil, S.J., 1988. Complete amino acid sequence of the thioesterase domain of chicken liver fatty acid synthase. Biochemistry 27, 7773–7777.

Yeung, L.Y., Young, E.D., Schauble, E.A., 2012. Measurements of $^{18}O^{18}O$ and $^{17}O^{18}O$ in the atmosphere and the role of isotope-exchange reactions. Journal of Geophysical Research 117, D18306.

Young, E.D., Galy, A., Nagahara, H., 2002. Kinetic and equilibrium mass-dependent isotope fractionation laws in nature and their geochemical and cosmochemical significance. Geochimica et Cosmochimica Acta 66, 1095–1104.

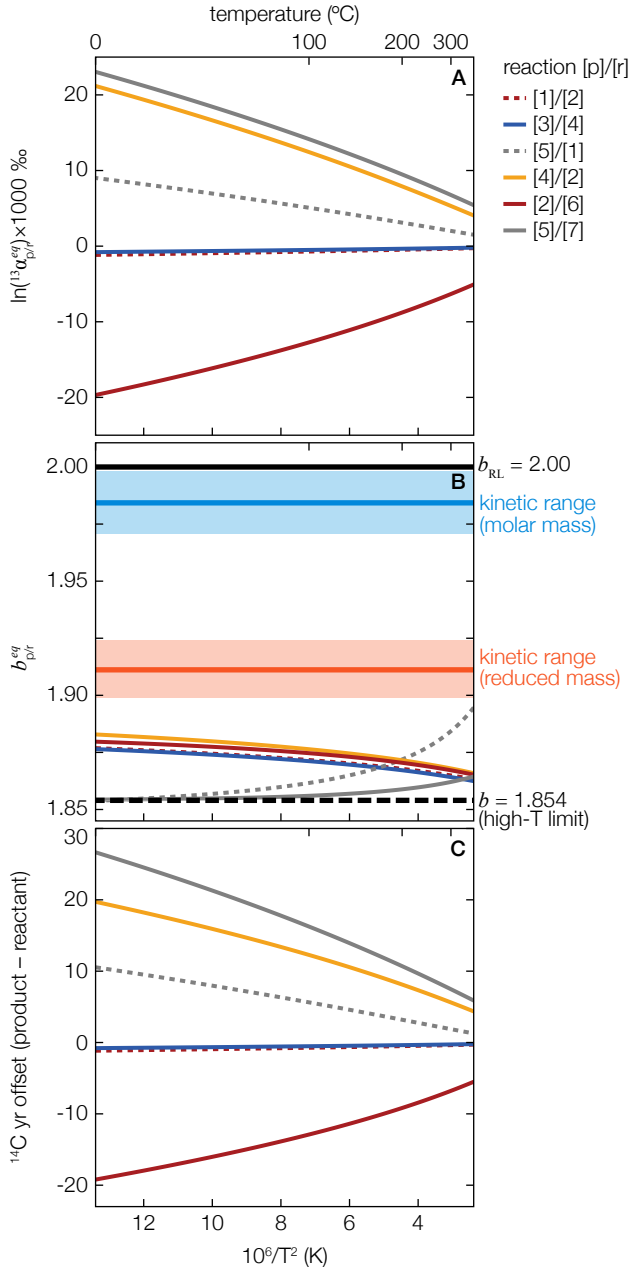

Figure 1: **Calculated isotope effects**. (**A**) $^{13}\alpha^{eq}_{p/r}$, (**B**) $b^{eq}_{p/r}$, and (**C**) ^{14}C age offsets for a suite of equilibrium reactions involving product (p) and reactant (r) compounds relevant for acetogenic lipid biosynthesis plotted as a function of reaction temperature. Compound numbers refer to: [1] = acetyl-ACP, [2] = acetyl-CoA, [3] = malonyl-ACP, [4] = malonyl-CoA, [5] = acetoacetyl-ACP, [6] = pyruvic acid, [7] = acetyl-ACP enolate, where CoA = coenzyme-A and ACP = acyl carrier protein (truncated at the phosphopantetheine group). Also shown in (**B**) are the predicted ranges of kinetic b values for all compounds reported in Table 2 ($\mu \pm 1\sigma$, $n = 11$) calculated using either their molar masses (i.e., diffusive processes) or their reduced masses (i.e., bond-breaking processes), as well as the high-temperature monoatomic equilibrium limit ($b = 1.854$) and the reference line value used to report all ^{14}C ages ($b_{RL} = 2.00$). Note that many of the reactions reported here are enzymatically catalyzed and thus do not operate in equilibrium in nature; nonetheless, equilibrium isotope effects represent a useful limiting case when exploring the possible range of ^{14}C age offsets due to fractionation.

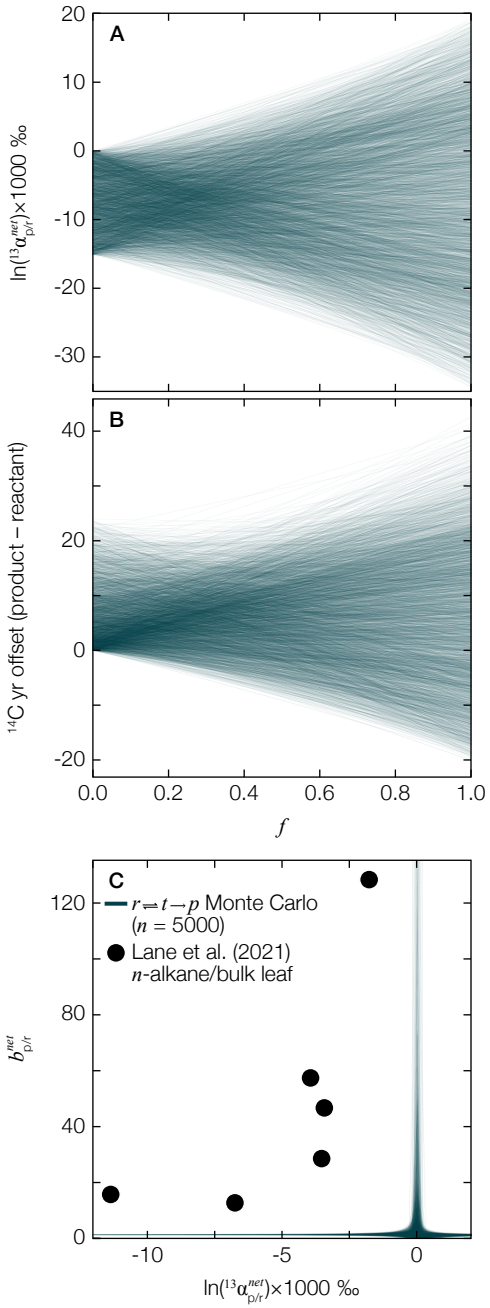

Figure 2: **Expressed isotope effects for a multi-step reaction network**. Monte Carlo results (n = 5000 iterations) for the reaction network $r \overset{\mathbf{1}}{\rightleftharpoons} t \overset{\mathbf{2}}{\longrightarrow} p$ showing (**A**) $^{13}\alpha^{net}_{\mathrm{p/r}}$ and (**B**) ^{14}C age offsets plotted as a function of f, the degree of reversibility for reaction step **1**, and (**C**) $b^{net}_{\mathrm{p/r}}$ plotted as a function of $^{13}\alpha^{net}_{\mathrm{p/r}}$. Also shown in panel (**C**) are the calculated b values for n-alkane biosynthesis relative to bulk leaf tissue that would be required to explain the ^{14}C results of Lane et al. (2021) (Table 1). These values are clearly inconsistent with Monte Carlo predictions, even when considering that the model calculations performed here encompass all known values for all input parameters (Section 2.4) and are therefore expected to yield the broadest possible b range. In contrast to the interpretation of Lane et al. (2021), these results indicate that non-canonical b values are only possible at "crossover points" when $\ln(^{13}\alpha_{net}) \rightarrow 0$, as has been reported previously for other isotope systems (Bao et al., 2015).